PHILOSOPHICAL TRANSACTIONS A

rsta.royalsocietypublishing.org

Research

**Cite this article:** Steinlechner J. 2018 Development of mirror coatings for gravitational- wave detectors. *Phil. Trans. R. Soc. A* **376**: 20170282.
http://dx.doi.org/10.1098/rsta.2017.0282

Accepted: 16 December 2017

One contribution of 11 to a discussion meeting issue 'The promises of gravitational-wave astronomy'.

**Subject Areas:**
optics, astrophysics

**Keywords:**
mirror coatings, thermal noise, optical absorption

**Author for correspondence:**
J. Steinlechner
e-mail: jessica.steinlechner@glasgow.ac.uk

# Development of mirror coatings for gravitational-wave detectors

J. Steinlechner[1,2]

[1]Institut für Laserphysik and Zentrum für Optische Quantentechnologien, Universität Hamburg, Luruper Chaussee 149, 22761 Hamburg, Germany
[2]SUPA, School of Physics and Astronomy, University of Glasgow, Glasgow G12 8QQ, UK

JS, 0000-0002-6697-9026

Gravitational waves are detected by measuring length changes between mirrors in the arms of kilometre-long Michelson interferometers. Brownian thermal noise arising from thermal vibrations of the mirrors can limit the sensitivity to distance changes between the mirrors, and, therefore, the ability to measure gravitational-wave signals. Thermal noise arising from the highly reflective mirror coatings will limit the sensitivity both of current detectors (when they reach design performance) and of planned future detectors. Therefore, the development of coatings with low thermal noise, which at the same time meet strict optical requirements, is of great importance. This article gives an overview of the current status of coatings and of the different approaches for coating improvement.

This article is part of a discussion meeting issue 'The promises of gravitational-wave astronomy'.

## 1. Introduction

Since 2015 several gravitational-wave signals have been detected by the Advanced LIGO[1] (aLIGO) and Advanced Virgo gravitational-wave detectors [1–5].

Gravitational waves cause extremely small distance changes—so small that typical gravitational waves

[1]This paper has LIGO document number LIGO-P1700347.



THE ROYAL SOCIETY PUBLISHING

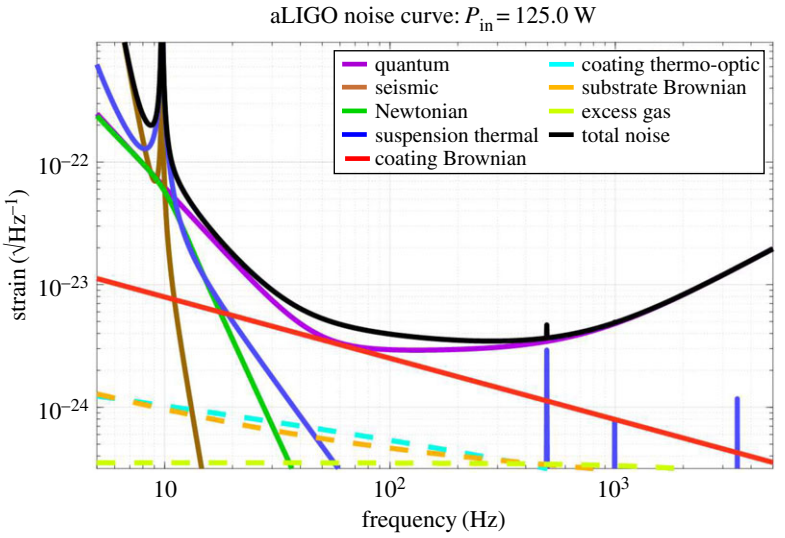


**Figure 1.** Design sensitivity of aLIGO simulated using a gravitational wave interferometer noise calculator (GWINC) (https://de.mathworks.com/company/newsletters/articles/confirming-the-first-ever-detection-of-gravitational-waves-by-analyzing-laser-interferometer-data.html): the black curve shows the total noise curve of the detector resulting from several of the different contributing noise sources shown in different colours. In the most sensitive part of the detection band between a few tens of hertz and a few hundreds of hertz, the detector will be limited by quantum noise (purple) and by coating thermal noise (red), which is a frequency-dependent noise source.

arriving on Earth cause changes comparable to changing the distance between the Earth and the Sun by less than the diameter of an atom. To detect gravitational waves, highly sensitive interferometers have been developed, which precisely measure the distance between suspended test masses coated to serve as highly reflective mirrors.

Thermal noise is a random vibration of a material's atoms and molecules due to its intrinsic temperature. Consequently, the mirrors forming the resonators in the arms of the gravitational-wave detectors vibrate due to thermal noise, and this can be shown to be dominated by the micrometre-thin coatings. This vibration translates into a movement of the mirrors' surfaces resulting in length changes of the detector arms, which limits our ability to see length changes due to gravitational waves.

Figure 1 shows the expected noise sources of aLIGO once it has reached design sensitivity [6,7]. In the most sensitive part of the detection band, thermal noise of the highly reflective mirror coatings shown by the red line limits the sensitivity of the detector, together with quantum noise [8]. A detailed description of the development and characterization of the coatings used in aLIGO and in Advanced Virgo is given by Granata *et al.* [9].

This article will give an overview of the parameters determining thermal noise of the mirror coatings and how these parameters can be changed and optimized to reduce coating thermal noise. In order to understand how to optimize coatings, the principle of how coatings work will be explained and an overview of currently used and potential future coating materials will be given.

## 2. Coating thermal noise

The coating thermal noise power spectral density can be described by

$$S_x(f) = \frac{2k_B T}{\pi^2 f Y_{sub}} \frac{d}{w^2} \left( \frac{Y_{coat}}{Y_{sub}} \phi_{\parallel} + \frac{Y_{sub}}{Y_{coat}} \phi_{\perp} \right), \tag{2.1}$$

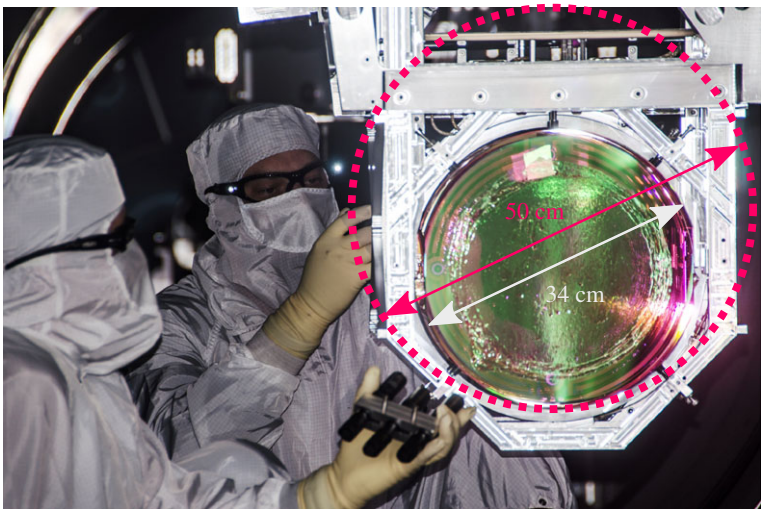


**Figure 2.** An aLIGO test-mass mirror 34 cm in diameter. (Photo: www.ligo.org.) The pink dotted circle indicates the proposed size of a mirror for the Einstein Telescope with a diameter of 50 cm. (Note that the mirror surface in the photo is covered by a protective film which makes it look rough.)

with $k_B$ being the Boltzmann constant, $T$ the mirror temperature, $Y$ the Young's modulus of the coating and substrate materials, $d$ the coating thickness, $w$ the radius of the laser beam on the coating, and $\phi_\parallel$ and $\phi_\perp$ the mechanical losses of the coating parallel and perpendicular to the coating layers [10].

A more complete model, in which the mechanical loss of each coating material is decomposed into losses associated with shear motion and with bulk motion, uses flexural (bulk) and shear loss instead of parallel and perpendicular loss [11,12]. However, this usually results in a very small correction factor, so, for ease of comparison with the existing body of thermal noise literature, the older model is used here.

Thermal noise is an effect depending on the frequency $f$ becoming more significant towards low frequencies. Gravitational-wave detection is sensitive to amplitude changes, not to intensity changes, which is why we chose to plot the amplitude spectral density of the thermal noise $\sqrt{S_x(f)}$.

## (a) The laser beam diameter

Thermal noise, $\sqrt{S_x(f)}$, is proportional to $1/w$ with $w$ being the beam diameter on the mirror surface, which means that thermal noise is reduced when averaging over a larger surface area. The laser beam has a Gaussian distribution with the radius being defined as the distance from the centre of the beam at which the intensity is decreased to $1/e^2 \approx 13.5\%$. The mirror diameter is chosen to be approximately $3 \times w$ to minimize optical losses due to the outer parts of the beam being outside the mirror.

The aLIGO mirrors are made of fused silica with a diameter of 34 cm, a thickness of 40 cm and a mass of 20 kg [6], as shown in figure 2, with a beam radius of 6.2 cm on the end mirrors of the interferometer arms [7]. For future gravitational-wave detectors, an increase in beam diameter is planned, e.g. the Einstein Telescope is being planned to have a diameter between 45 cm and 62 cm [13]. The pink dotted line in figure 2 shows a diameter of about 50 cm resulting in a possible beam diameter increase and consequently a sensitivity increase by a factor of about $\sqrt{2}$. From the perspective of material development, the restrictions on the mirror size are the availability of large substrates and the ability to produce large-scale coatings with the required homogeneity.

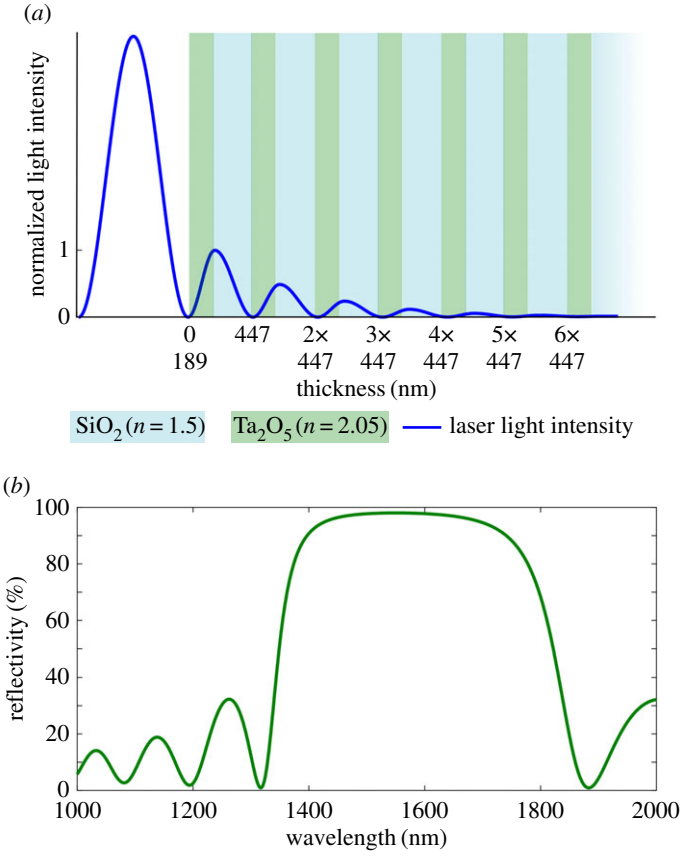


**Figure 3.** (*a*) Light intensity (blue line) inside a highly reflective multi-layer coating made of 13 layers, which are each a quarter of a wavelength in optical thickness, of two alternating materials ($SiO_2$ in blue and $Ta_2O_5$ in green) on a $SiO_2$ substrate (fading blue on the right side). The light field is entering the coating from the left side from an air or vacuum environment. (*b*) Reflectivity of the coating in per cent as a function of laser wavelength. The reflectivity maximizes at the design wavelength of 1550 nm.

**Table 1.** Mechanical loss $\phi$ at different temperatures of the materials discussed.

| | loss $\phi \times 10^{-4}$ | | | |
|---|---|---|---|---|
| | $SiO_2$ | Ti:$Ta_2O_5$ | *a*-Si | $SiN_x$ |
| 290 K | 0.4 [21] | 2.4 [21] | 1.0 (IBS) [22] | 0.8 [23] |
| 120 K | 1.7 [24] | 3.3 [25] | 0.8 (IBS) [22] | 0.2 [23] |
| 20 K | 7.8 [24] | 8.6 [25] | 0.2 (IBS) [22] | 0.1 [23] |

## (b) Coating thickness

The thickness of the coating depends on the reflectivity required and on the refractive index of the coating materials.

Highly reflective coatings are made of alternating layers of two materials with different refractive indices. The reflectivity of the coating maximizes (for a minimum number of layers) when the layers have an optical thickness of refractive index $n$ multiplied by the geometric thickness $t$ of a quarter of a wavelength $\lambda$ and the layer on top of the coating is made of the material with higher refractive index. Note that in reality there are often reasons for using a

more complicated coating design; for example, the aLIGO design differs from ideal quarter-wavelength-thick layers to achieve a certain reflectivity at two wavelengths. By adjusting the thickness of the layers, thermal noise can also be reduced [14,15]. An approximation of the (intensity) reflectivity $R$ of a coating in air or vacuum made of two materials with refractive index $n_H$ and $n_L$ on a substrate with refractive index $n_S$ can be made using [16]

$$R_{2N} = \left( \frac{n_S (n_H/n_L)^{2N} - 1}{n_S (n_H/n_L)^{2N} + 1} \right)^2 \quad \text{and} \quad R_{2N+1} = \left( \frac{n_H^2 (n_H/n_L)^{2N} - n_S}{n_H^2 (n_H/n_L)^{2N} + n_S} \right)^2. \tag{2.2}$$

A combination of one low and one high refractive layer is also called a bilayer so that $R$ is a function of $N$, with $N$ being the number of bilayers and $2N$ the number of single layers for an even number of layers (equation $(2.2)_1$). For an uneven number of layers, $2N + 1$, the equation changes into equation $(2.2)_2$. These equations also show that $R$ increases for an increasing ratio $n_H/n_L$ and, therefore, that for a larger $n_H/n_L$ fewer bilayers are required to achieve a certain $R$.

Figure 3*a* shows a multi-layer coating made of $2N + 1 = 13$ alternating layers of $SiO_2$ ($n_L = 1.5$, blue) and $Ta_2O_5$ ($n_H = 2.05$, green) on a fused silica substrate ($n_S = 1.5$, blue). The dark blue line shows the laser light intensity for a light field coming from the left. Using equation (2.2), this results in a reflectivity of $R = 96.69\%$. Figure 3*b* shows the reflectivity of the coating as a function of wavelength calculated using (https://github.com/sestei/dielectric) based on beam transfer matrix formalism. This more accurate way to calculate the reflectivity also results in $R = 96.66\%$ at the design wavelength of 1550 nm.

While the refractive indices of the coating materials determine the coating thickness, the possible variations in thickness are small compared with the effect other properties such as mechanical loss or optical absorption (discussed in the following sections) can have on the coating performance.

## (c) Mechanical loss of the coating materials

Mechanical loss is related to the atomic-scale structure of the amorphous coating materials and significant research is focused on understanding the microscopic mechanisms responsible for the mechanical loss. For example, it appears that changes in the medium range atomic ordering in $Ta_2O_5$ are strongly correlated with changes in the mechanical loss [17]. Computational atomic modelling studies have begun to obtain good agreement with experimental measurements [18,19].

Thermal noise, $\sqrt{S_x(f)}$, is proportional to the square root of the mechanical loss $\phi$, which is a material property. Mechanical loss, or internal friction, is the phase lag between a stress applied to a material and the resulting strain. For a resonant system, the mechanical loss is the inverse of the quality factor of the resonance and how much of the energy stored in a vibrational mode is dissipated with each cycle of oscillation. A detailed derivation of coating thermal noise showing its relationship to mechanical loss is given by Harry *et al*. [10] and Levin [20].

Table 1 shows the mechanical loss of $SiO_2$- and $TiO_2$-doped $Ta_2O_5$ (Ti:$Ta_2O_5$), the coating materials used in the coatings of aLIGO, at different temperatures. From table 1 we can see the following.

— At room temperature (290 K), the mechanical loss of Ti:$Ta_2O_5$ is significantly larger than that of $SiO_2$. It was first shown by Penn *et al*. in 2003 [26] that $Ta_2O_5$ dominates the total mechanical loss of the coating and, therefore, replacing or improving $Ta_2O_5$ has priority to reduce coating thermal noise at room temperature.
— The mechanical loss of both materials increases with decreasing temperature.
— At 20 K, the mechanical loss of $SiO_2$ and Ti:$Ta_2O_5$ is almost equal and, therefore, coating improvement has to be concentrated not only on Ti:$Ta_2O_5$, but on both materials for future cryogenic detectors such as the Einstein Telescope.

For comparison, table 1 also shows the mechanical loss of amorphous silicon (*a*-Si)—a material with very different behaviour: the mechanical loss of *a*-Si deposited using the ion beam sputtering (IBS)-coating deposition technique is between the losses of $SiO_2$ and Ti:$Ta_2O_5$ at room temperature, but decreases towards lower temperatures resulting in a mechanical loss 40× below the mechanical loss of Ti:$Ta_2O_5$ at 20 K.

## (d) Temperature of the test-mass mirror

Reducing the test-mass temperature is, in principle, a straightforward way to reduce coating thermal noise. The Japanese detector KAGRA will be the first cryogenically operated detector with a target temperature of about 20 K [27]. Future detectors, such as the Einstein Telescope and LIGO Voyager, are also planning to operate at low temperatures [13,28].

Fused silica, the currently used test-mass substrate material, has a very low mechanical loss at room temperature, which increases by several orders of magnitude at cryogenic temperatures [29]. The resulting thermal noise at low temperatures would be higher than at room temperature due to the mechanical loss increase. Alternative materials with a low mechanical loss at low temperatures are sapphire or crystalline silicon. KAGRA uses sapphire, which is transparent at a wavelength of 1064 nm. For the Einstein Telescope and for upgrades to aLIGO, silicon is planned to be used. Silicon shows properties that gravitational-wave detectors will benefit from, such as a very high thermal conductivity and zero thermal expansion at 18 K and at 120 K, which makes these temperatures very interesting due to low thermo-elastic noise [30]. Silicon is not transparent at 1064 nm. Therefore, silicon test masses require a change in wavelength to greater than or equal to 1450 nm to keep optical absorption low. Of particular interest is the telecommunication wavelength of 1550 nm due to available high-power lasers and optical components. Note that a wavelength change results in a changed coating thickness.

A temperature reduction from 290 K to 20 K would reduce coating thermal noise by a factor of $\sqrt{290/20} \approx 4$, if the parameters remain unchanged. As table 1 shows, the mechanical loss of $SiO_2$ and Ti:$Ta_2O_5$ increases when the materials are cooled (see §2c). As a consequence, coating thermal noise improves less than expected from the temperature reduction and cooling the test masses to 20 K would result in a thermal noise decrease by a factor of only about 2. Figure 4 shows the thermal noise improvement when cooling the coatings compared with the theoretical improvement which could be achieved from cooling, if mechanical loss remained at its room temperature value. While coating thermal noise still benefits from cooling $SiO_2$ and Ti:$Ta_2O_5$, the improvement is not sufficient for the requirements of future gravitational-wave detectors. Cryogenic mechanical loss measurements on $SiO_2$ and $Ta_2O_5$ multi-layer coatings confirm a too high mechanical loss for future gravitational-wave detectors [33].

## (e) Optical absorption

The optical absorption is not related to coating thermal noise, but forms an important restriction for material selection. The requirement on the optical absorption of a highly reflective multi-layer coating for current and future detectors is of the order of ppm ($10^{-6}$) [7,13].

For current detectors operated at room temperature, the main issue with coating (and substrate) absorption is heating of the fused silica test masses with the profile of the Gaussian laser beam. Owing to a low thermal conductivity, thermal lensing, which is a thermal expansion of the substrate ($a_{\mathrm{th}}$) and a change of the refractive index with temperature ($\mathrm{d}n/\mathrm{d}T$), forms a so-called thermal lens that causes beam distortions.

Crystalline silicon is considered to be a substrate material for cryogenically operated detectors because of a low mechanical loss at low temperatures. Silicon has a very high thermal conductivity. Therefore, thermal lensing due to optical absorption is less of an issue than for room temperature detectors. However, optical absorption increases the test-mass temperature. In vacuum and at low temperature, the only option to cool the test masses is through the very

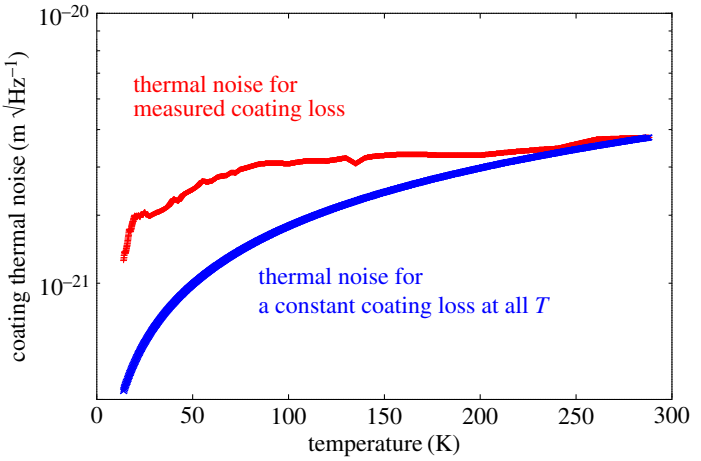


**Figure 4.** Coating thermal noise at 100 Hz. The blue (lower) line shows the calculated coating thermal noise for a coating at cryogenic temperatures, assuming the coating parameters remained constant at their room temperature values. The real improvement of a coating made of $SiO_2$ and Ti:$Ta_2O_5$ is shown by the (upper) red line, which takes a mechanical loss increase in the coating materials into account [31,32]. (Online version in colour.)

thin mirror suspensions [34]. Therefore, optical absorption has to be minimized to maintain the low temperature of the test masses.

## 3. Coatings and coating materials

### (a) Current coating materials

$SiO_2$ and Ti:$Ta_2O_5$ are the coating materials that are currently used in gravitational-wave detectors. The deposition method used is IBS. While the optical absorption of these coatings is very low [35], the mechanical loss has been under continuous investigation since the early 2000s [26].

In 2006, it was found that the mechanical loss reduces by 40% when doping $Ta_2O_5$ with 22.5% $TiO_2$ [36]. Therefore, aLIGO and Advanced Virgo use Ti:$Ta_2O_5$ in combination with $SiO_2$, while the initial detectors used undoped $Ta_2O_5$.

The room temperature mechanical loss of (undoped) $Ta_2O_5$ deposited via IBS decreases with heat treatment at temperatures of up to 600°C, while for heat treatment at higher temperatures cryogenic mechanical loss peaks develop [37].

As described in §2b, in the simplest case, the coating layers in a highly reflective coating are each a quarter of a wavelength in optical thickness. Such a design achieves the highest reflectivity with a minimum number of layers and therefore minimal coating thickness, but, in the case of an unequal thermal noise contribution of the two materials (e.g. for $SiO_2$ and Ti:$Ta_2O_5$), thermal noise can benefit from an optimized design with a higher content of the low mechanical loss material [14,15].

### (b) Amorphous silicon: an amorphous high-index alternative

Amorphous silicon (*a*-Si) has a low mechanical loss [38], which decreases towards low temperatures (table 1). The very high refractive index of *a*-Si of between 3.5 and 4.0 (varying with deposition parameters) would reduce the number of layers required to achieve high reflectivity and the thickness of the layers.

The high refractive index makes *a*-Si a possible replacement material for Ti:$Ta_2O_5$. A coating made of *a*-Si and $SiO_2$ would reduce coating thermal noise by a factor of 2 compared with $SiO_2$ and Ti:$Ta_2O_5$ at 20 K due to the lower mechanical loss and the reduction in coating thickness. However, the optical absorption of *a*-Si at 1550 nm has been shown to be about 1000 ppm for a highly reflective *a*-Si/$SiO_2$ coating and therefore too high for application in gravitational-wave detectors. There has been a lot of research into absorption reduction of *a*-Si over past years and is still ongoing.

— It has been shown that commercial *a*-Si coatings produced with the IBS method (deposition method used for $SiO_2$ and Ti:$Ta_2O_5$ coatings in current GW detectors) show high optical absorption at 1550 nm of the order of up to a few per cent at 1550 nm in an as- deposited state [39,40].
— Coatings produced with different deposition techniques show different optical absorption in an as-deposited state. Coatings produced with the ion plating procedure [41] have a significantly lower optical absorption after deposition than those deposited via IBS [40] of about 1000 ppm [42].
— The optical absorption significantly reduces (by $\approx 80\%$) with heat treatment showing a minimum at a certain temperature [40], which varies between 400°C and 500°C for different vendors and deposition methods.
— The optical absorption of *a*-Si at 1064 nm is significantly higher than that at 1550 nm [40]. The exact factor varies for coatings from different vendors and depends on parameters such as heat treatment.
— The optical absorption of IBS coatings has been shown to reduce by nearly a factor of 2 when cooling the mirror [40].
— Recent results indicate significant absorption reduction to be possible when using a higher wavelength [43] and when optimizing the deposition procedure [44].

It has been shown that elevated temperature deposition can significantly reduce the mechanical loss of *a*-Si compared with the usual procedure of deposition at, or slightly above, room temperature and post-deposition annealing [45]. This is thought to be an example of forming an 'ideal glass' [46]. In such a material, the atoms are arranged in a low-energy configuration resulting in a low mechanical loss. To realize such a configuration, the material has to be deposited extremely slowly or, alternatively, at a high substrate temperature to provide energy for the atoms to rearrange until the next layer of atoms is deposited. The effect of deposition at high temperatures on the optical absorption of *a*-Si is currently under investigation.

## (c) Silicon nitride: an amorphous low-index alternative

Thermal noise of an *a*-Si/$SiO_2$ coating at low temperature would be dominated by the mechanical loss of the $SiO_2$ layers. The high refractive index of *a*-Si allows the possible use of a wide range of materials as the lower refractive index partner material in the coating. One option is silicon nitride ($SiN_x$, where $x$ indicates varying stoichiometry), which also has very low mechanical loss at low temperatures (table 1) [23]. Based on the literature values for mechanical loss, and on the required thickness for such a coating, the thermal noise of an *a*-Si and SiN coating is likely to be more than an order of magnitude below the thermal noise of a $SiO_2$ and Ti:$Ta_2O_5$ coating at 20 K.

Detailed investigations of SiN deposited via plasma-enhanced chemical vapour deposition (PECVD) have shown that the exact material composition has a strong effect on the material properties, e.g. on the optical absorption, the refractive index and the mechanical loss [47], with evidence of lower mechanical losses than current GW-coating materials at room temperature and at low temperature down to 10 K [48,49]. The optical absorption of a SiN/$SiO_2$ is similar to the best *a*-Si/$SiO_2$ [47,50]. The varying refractive index for varying compositions of SiN could potentially also allow the option of a pure SiN coating in which SiN forms the high and low refractive index layers.

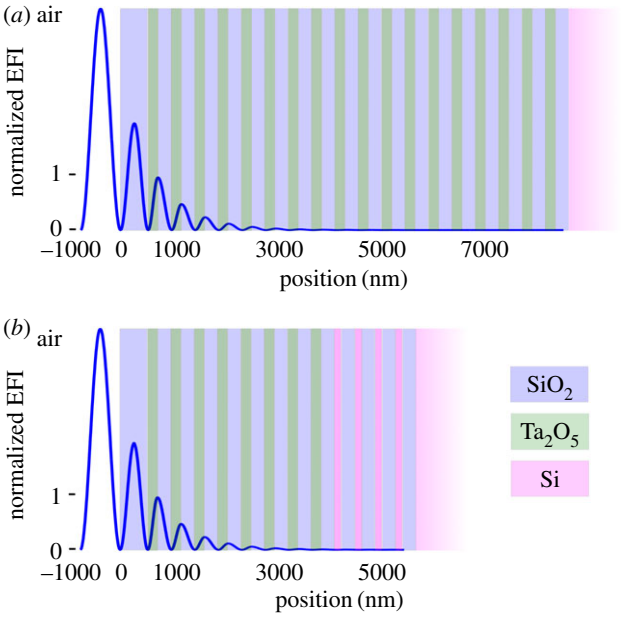


**Figure 5.** (*a*) Schematic of a highly reflective multi-layer coating, which consists of 18 bilayers of $SiO_2$ (blue) and Ti:$Ta_2O_5$ (green) on a Si (pink) substrate. The blue line shows the (normalized) laser light intensity (EFI) in the coating, which decreases by about 50% with every bilayer. (*b*) Schematic of a multi-material coating identical in reflectivity, in which the first eight bilayers are made of $SiO_2$ and Ti:$Ta_2O_5$, while in the lowest four bilayers the Ti:$Ta_2O_5$ layers are replaced by *a*-Si.

## (d) Multi-material coatings

An option to use too high absorbing materials in a coating to exploit their low mechanical loss is through multi-material coatings [51,52], in which more than two materials are combined. In these designs, materials with low mechanical loss but high optical absorption are used in lower coating layers, in which the laser power is reduced, to keep the total optical absorption low. The lower the optical absorption, the closer to the top of the coating a material can be used.

Figure 5*a* shows an example of a $SiO_2$ and Ti:$Ta_2O_5$ coating with high reflectivity (about 5 ppm transmission). Such a coating has been measured to have an optical absorption of 1.7 ppm at 1550 nm [51].

For the refractive indices of $SiO_2$ and Ti:$Ta_2O_5$, the incident laser power reduces by almost exactly 50% after each bilayer, so that after eight bilayers $(0.5)^8 \approx 0.4\%$ of the incident power is left. In figure 5*b*, after the first eight bilayers, the Ti:$Ta_2O_5$ layers are replaced by low mechanical loss, but high absorbing *a*-Si. Assuming the high optical absorption of the early *a*-Si/$SiO_2$ coatings of 1000 ppm, these 1000 ppm would be reduced to 0.4% of 1000 ppm = 4 ppm due to the $SiO_2$ and Ti:$Ta_2O_5$ layers on top. Therefore, the total coating absorption would be (1.7 + 4) ppm = 5.7 ppm, while the coating would benefit from the low mechanical loss of the *a*-Si layers and, even more, from the high refractive index, which makes it possible to use a much smaller total number of layers than in a 'pure' $SiO_2$ and Ti:$Ta_2O_5$ coating. At 20 K, this coating would reduce thermal noise by 20%.

In the example of $SiO_2$ and Ti:$Ta_2O_5$ with a power reduction of 50% per bilayer, it is easy to see that, with each absorption reduction by a factor of 2 in the *a*-Si part of the coating, one fewer bilayer of $SiO_2$ and Ti:$Ta_2O_5$ is needed to keep the optical absorption low.

This idea can be extended to using even more than three materials [50] or to concentrating on improving the top layer of the coating [53].

## (e) Nano-layer coatings: a way to adjust the crystallization temperature

The concept of nano-layers divides a single layer inside a multi-layer coating into a sub-structure of much thinner layers (the refractive index of the layer is then an average of the refractive indices of the two materials weighted with their thickness). Substructures of up to 19 sub-layers of $TiO_2$ and $SiO_2$ forming one quarter-wave layer have been tested with a thickness of less than 10 nm per sub-layer [54]. Such a sub-structure can prevent the material from crystallizing due to heat treatment. In the example of $TiO_2$, the crystallization temperature has been increased by more than 50°C (from 250°C to > 300°C) due to the $SiO_2$ layers.

Nano-layers may allow the benefits from possible improvements in optical absorption and/or mechanical loss at higher heat treatment temperatures than usually possible due to poly-crystalline structures forming, which cause an optical absorption and mechanical loss increase and high optical scattering.

A possible adjustment of the crystallization temperature is of particular interest for multi-layer coatings made of two or even more materials as the optimum heat treatment temperature varies for different materials, and optimum treatment for each of the materials is currently often not easily possible. A good example is an *a*-Si and $SiO_2$ coating in which the *a*-Si component ideally needs heat treatment at about 450°C to minimize the optical absorption, while the mechanical loss of $SiO_2$ reduces up to 600°C.

## (f) Crystalline coatings

Many amorphous materials show characteristic mechanical loss peaks at low temperatures associated with their disordered structure [29,55,56], while, by contrast, crystalline materials can show much lower mechanical loss at low temperatures. It is possible to epitaxially grow mono-crystalline highly reflective multi-layer coatings. However, to grow a mono-crystalline coating, the lattice structures and constants of the substrate material and of the two coating materials have to be matched. Two combinations have been investigated within the gravitational-wave community over the past years: GaAs/AlGaAs [57] and GaP/AlGaP [58–60].

### (i) GaAs/AlGaAs

A system made of AlGaAs and GaAs layers can be grown on GaAs wafers. The mechanical loss of such a coating is about $5.4 \times 10^{-6}$ at 20 K [61] and the thickness of a highly reflective coating is about 9.6 µm instead of 6.8 µm for $SiO_2$ and Ti:$Ta_2O_5$. The resulting thermal noise is about 10 times lower than that for an equivalent $SiO_2$ and Ti:$Ta_2O_5$ coating.

The optical absorption of AlGaAs has been shown to be homogeneous and linear within the intensity range of interest for gravitational-wave detectors [62], and over recent years there has been an absorption improvement [62,63], which makes AlGaAs an attractive option for use in experiments with strict optical and mechanical requirements.

GaAs is not a suitable substrate material for most of these applications, but a substrate transfer procedure to substrates made of silicon or fused silica has been developed. The drawback for the use of AlGaAs coatings in future gravitational-wave detectors is the maximum available size of the GaAs wafers to grow the coatings on, which is currently limited to about 20 cm. The development of larger GaAs substrates or an alternative suitable substrate material would be required to produce AlGaAs coatings in the sizes planned for future gravitational-wave detectors [63].

### (ii) GaP/AlGaP

Crystalline coatings made of GaP and AlGaP are an interesting alternative to AlGaAs as they can be grown on crystalline silicon [58–60]. This would solve the size problem for gravitational-wave detectors and make even the substrate transfer, which involves a bonding procedure, unnecessary. The mechanical loss of a GaP/AlGaP multi-layer coating has been shown to be $2.5 \times 10^{-5}$ (on

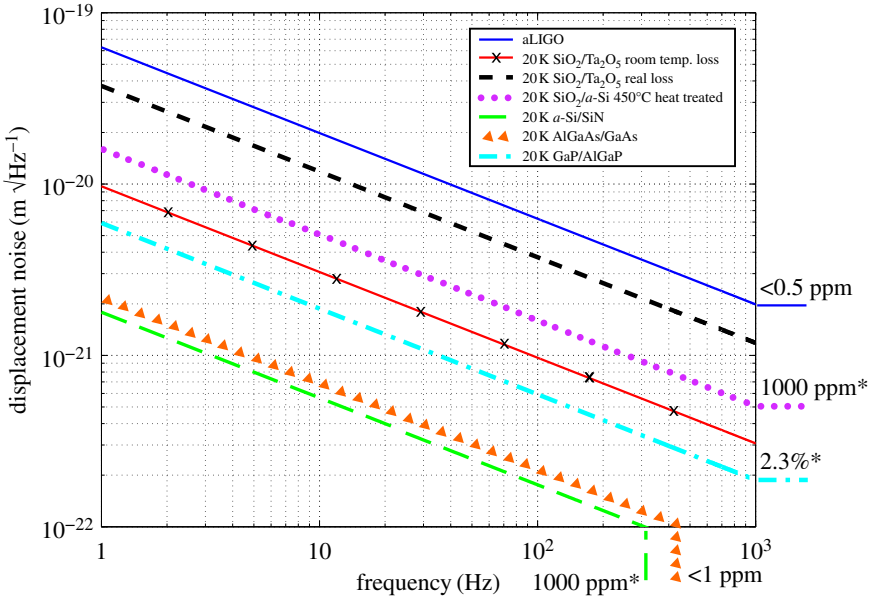


**Figure 6.** Overview of the current status of coating thermal noise performance and optical absorption of the coating materials discussed in this article. In this plot, displacement noise (or amplitude spectral density of the thermal noise $\sqrt{S_x(f)}$) of the highly reflective-coated end mirrors in the detector's arm cavities is shown. *Work on reducing the optical absorption of GaP/AlGaP and *a*-Si is currently in progress.

average) at 20 K [59], which is significantly lower than the mechanical loss of $SiO_2$ and Ti:$Ta_2O_5$ (approx. $8 \times 10^{-4}$). A GaP/AlGaP coating would have to be about a factor of 2 thicker than $SiO_2$ and Ti:$Ta_2O_5$ [59]. The resulting thermal noise would be about a factor of 4 below thermal noise of an equivalent $SiO_2$ and Ti:$Ta_2O_5$ coating at 20 K.

An initial coating had a high absorption of 2.3% [64]. The history of AlGaAs has shown significant reduction in optical absorption by reducing impurities in the coating materials. Therefore, there might be scope for significant improvement of GaP. Further development of GaP coatings is planned.

## 4. Conclusion

Figure 6 shows an overview of the materials discussed in this article. The plot shows the displacement noise of the highly reflective-coated end mirrors in the detector's arm cavities.[2]

— The blue (top) line shows the thermal noise performance of the coatings made of $SiO_2$ and Ti:$Ta_2O_5$ currently used in aLIGO at room temperature, on a $SiO_2$ substrate and for the currently used beam radius of 6 cm. Such coatings show low optical absorption of less than 0.5 ppm and, in theory, can be upscaled to the size required by future gravitational-wave detector designs.
— The red line marked with X's shows the theoretical thermal noise performance, reduced by a factor of 6 compared with room temperature, of these coatings when cooling them to 20 K assuming their material properties were to remain unchanged at their room temperature values. For this case (and all cryogenic calculations in this figure), a silicon

[2]This compares to the aLIGO sensitivity shown in figure 1 by dividing the displacement noise by the detector's arm length and taking the number of mirrors in the detector into account. Thermal noise of the mirrors adds in quadrature as their noise is uncorrelated. Also the cavity input mirrors have a lower reflectivity than the end mirrors and, therefore, lower thermal noise.

substrate and a beam diameter of 9 cm were used such as planned in design for future gravitational-wave detectors.

— The real thermal noise is shown by the black line (short dashes, second from the top) as the material properties do change with cooling in a way that the mechanical loss increases significantly. Thermal noise still improves by more than a factor of 2 compared with room temperature, but this is too small an improvement for future gravitational-wave detectors, meaning a significant limitation due to thermal noise in the most sensitive part of the detection band.

— Replacing Ti:$Ta_2O_5$ by *a*-Si would reduce thermal noise by another factor of 2, resulting in the purple (dotted) line. Such a coating would have a too high optical absorption due to the *a*-Si, but current research concentrates on absorption reduction. An (additional) option to keep the optical absorption low would be a multi-material coating in which only a few of the Ti:$Ta_2O_5$ layers are replaced by *a*-Si. The number of replaced layers and the achievable thermal noise reduction is a trade-off between thermal noise reduction and tolerable optical absorption.

— Replacing Ti:$Ta_2O_5$ by *a*-Si would make coating thermal noise to be limited by the mechanical loss of the $SiO_2$ in the coating. SiN would be an option for a low-index material in combination with *a*-Si. The optical absorption of SiN is negligible compared with the absorption in *a*-Si. Thermal noise of such a coating would be more than an order of magnitude lower than that of a cooled aLIGO coating shown by the green line (long dashes, bottom).

— Crystalline coatings are an interesting alternative to amorphous coatings with AlGaAs showing a coating thermal noise very similar to *a*-Si/SiN (orange triangles, second from the bottom), while even the optical absorption of AlGaAs would be within the requirements for use in gravitational-wave detectors. The size of AlGaAs coatings is currently limited to a maximum of about 20 cm due to the availability of GaAs wafers to grow the coatings on, which is about a factor of 2.5 too small for future gravitational-wave detectors.

— Another crystalline option is GaP, shown by the light blue (dashes and dots, third from the bottom) line. A factor of 4 in thermal noise decrease compared with a cooled aLIGO coating makes GaP a very attractive material, in particular as GaP can theoretically be upscaled to the required sizes as it can be grown on Si. However, further research into absorption reduction will be required to make GaP suitable for application in future detectors.

This article gives an overview of the main options currently being investigated to find a way to reduce coating thermal noise in future gravitational-wave detectors. This continues to be an active area of research. It seems likely that one of these options, or a combination of several, will contribute to the reduction of coating thermal noise in future detectors, but there may also be further, different approaches possible.

Data accessibility. This article has no additional data.

Competing interests. The author declares no competing interests.

Funding. The author is grateful for the financial support provided by STFC (ST/L000946/1), the University of Glasgow and Universität Hamburg.

Acknowledgements. The author thanks the following people for their help and valuable input to the manuscript: R. Birney, G. Cagnoli, G. Harry, B. Lantz, I. Martin, F. Schiettekatte, R. Schnabel, L. Terkowski. The author also thanks the referees and the editor.

## References

1. Abbott BP *et al.* 2016 Observation of gravitational waves from a binary black hole merger. *Phys. Rev. Lett.* **116**, 061102. (doi:10.1103/PhysRevLett.116.061102)

2. Abbott BP *et al.* 2016 GW151226: observation of gravitational waves from a 22-solar-mass binary black hole coalescence. *Phys. Rev. Lett.* **116**, 241103. (doi:10.1103/PhysRevLett.116.241103)
3. Abbott BP *et al.* 2017 GW170104: observation of a 50-solar-mass binary black hole coalescence at redshift 0.2. *Phys. Rev. Lett.* **118**, 221101. (doi:10.1103/PhysRevLett.118.221101)
4. Abbott BP *et al.* 2017 GW170814: a three-detector observation of gravitational waves from a binary black hole coalescence. *Phys. Rev. Lett.* **119**, 141101. (doi:10.1103/PhysRevLett.119.141101)
5. Abbott BP *et al.* 2017 GW170817: observation of gravitational waves from a binary neutron star inspiral. *Phys. Rev. Lett.* **119**, 161101. (doi:10.1103/PhysRevLett.119.161101)
6. Abbott BP *et al.* 2016 GW150914: the advanced LIGO detectors in the era of first discoveries. *Phys. Rev. Lett.* **116**, 131103. (doi:10.1103/PhysRevLett.116.131103)
7. Abbott BP *et al.* 2015 Advanced LIGO. *Class. Quantum Grav.* **32**, 074001. (doi:10.1088/0264-9381/32/7/074001)
8. Heurs M. 2018 Gravitational wave detection using laser interferometry beyond the standard quantum limit. *Phil. Trans. R. Soc. A* **376**, 20170289. (doi:10.1098/rsta.2017.0289)
9. Granata M *et al.* 2016 Mechanical loss in state-of-the-art amorphous optical coatings. *Phys. Rev. D* **93**, 012007. (doi:10.1103/PhysRevD.93.012007)
10. Harry GM *et al.* 2002 Thermal noise in interferometric gravitational wave detectors due to dielectric optical coatings. *Class. Quantum Gravity* **19**, 897. (doi:10.1088/0264-9381/19/5/305)
11. Hong T, Yang H, Gustafson EK, Adhikari RX, Chen Y. 2013 Brownian thermal noise in multilayer coated mirrors. *Phys. Rev. D* **87**, 082001. (doi:10.1103/PhysRevD.87.082001)
12. Abernathy M *et al.* 2017 Bulk and shear mechanical loss of titania-doped tantala. *Phys. Lett. A*. (doi:10.1016/j.physleta.2017.08.007)
13. Abernathy M *et al.* 2011 *Einstein Gravitational Wave Telescope (ET) conceptual design study: ET-0106C-10*. Cascina, Italy: European Gravitational Observatory. See https://tds.ego-gw.it/ql/?c=7954.
14. Villar AE *et al.* 2010 Measurement of thermal noise in multilayer coatings with optimized layer thickness. *Phys. Rev. D* **81**, 122001. (doi:10.1103/PhysRevD.81.122001)
15. Principe M. 2015 Reflective coating optimization for interferometric detectors of gravitational waves. *Opt. Express* **23**, 10 938–10 956. (doi:10.1364/OE.23.010938)
16. Heavens OS. 1970 *Thin film physics*. London, UK: Methuen.
17. Hart MJ, Bassiri R, Borisenko KB, Veron M, Rauch EF, Martin IW, Rowan S, Fejer MM, MacLaren I. 2016 Medium range structural order in amorphous tantala spatially resolved with changes to atomic structure by thermal annealing. *J. Non. Cryst. Solids* **438**, 10–17. (doi:10.1016/j.jnoncrysol.2016.02.005)
18. Trinastic JP, Hamdan R, Billman C, Cheng HP. 2016 Molecular dynamics modeling of mechanical loss in amorphous tantala and titania-doped tantala. *Phys. Rev. B* **93**, 014105. (doi:10.1103/PhysRevB.93.014105)
19. Billman CR, Trinastic JP, Davis DJ, Hamdan R, Cheng HP. 2017 Origin of the second peak in the mechanical loss function of amorphous silica. *Phys. Rev. B* **95**, 014109. (doi:10.1103/PhysRevB.95.014109)
20. Levin Y. 1998 Internal thermal noise in the LIGO test masses: a direct approach. *Phys. Rev. D* **57**, 659. (doi:10.1103/PhysRevD.57.659)
21. Flaminio R, Franc J, Michel C, Morgado N, Pinard L, Sassolas B. 2010 A study of coating mechanical and optical losses in view of reducing mirror thermal noise in gravitational wave detectors. *Class. Quantum Grav.* **27**, 084030. (doi:10.1088/0264-9381/27/8/084030)
22. Murray PG, Martin IW, Abernathy MR, Craig K, Hough J, Pershing T, Penn S, Robie R, Rowan S. 2015 Ion-beam sputtered amorphous silicon films for cryogenic precision measurement systems. *Phys. Rev. D.* **92**, 062001. (doi:10.1103/PhysRevD.92.062001)
23. Liu X, Metcalf TH, Wang Q, Photiadis DM. 2007 Elastic properties of several silicon nitride films. In *Proc. of Symposium A: Amorphous and Polycrystalline Thin-Film Silicon Science and Technology, San Francisco, CA, 9–13 April 2007* (eds V Chu, S Miyazaki, A Nathan, J Yang, H-W Zan). Materials Research Society Symposium Proceedings, vol. 989, pp. 511. New York, NY: Cambridge University Press.
24. Martin IW. 2009 Studies of materials for use in future interferometric gravitational wave detectors. PhD Thesis, University of Glasgow, Glasgow, UK.

25. Martin IW *et al.* 2009 Comparison of the temperature dependence of the mechanical dissipation in thin films of $Ta_2O_5$ and $Ta_2O_5$ doped with $TiO_2$. *Class. Quantum Gravity* **26**, 155012. (doi:10.1088/0264-9381/26/15/155012)
26. Penn SD *et al.* 2003 Mechanical loss in tantala/silica dielectric mirror coatings. *Class. Quantum Gravity* **20**, 2917–2928. (doi:10.1088/0264-9381/20/13/334)
27. Aso Y, Michimura Y, Somiya K, Ando M, Miyakawa O, Sekiguchi T, Tatsumi D, Yamamoto H. 2013 Interferometer design of the KAGRA gravitational wave detector. *Phys. Rev. D* **88**, 043007. (doi:10.1103/PhysRevD.88.043007)
28. Adhikari R. 2012 LIGO III Blue ConceptLIGO. Technical Document LIGO-G1200573. See dcc.ligo.org/LIGO-G1200573-v1/public.
29. Topp K, Cahill DG. 1996 Elastic properties of several amorphous solids and disordered crystals below 100 K. *Z. Phys. B* **101**, 235–245. (doi:10.1007/s002570050205)
30. Rowan S, Byer RL, Fejer MM, Route R, Cagnoli G, Crooks DRM, Hough J, Sneddon PH, Winkler W. 2003 Test mass materials for a new generation of gravitational wave detectors. *Proc. SPIE* **4856**, 292–297. (doi:10.1117/12.459019)
31. Martin IW. 2010 Talk at the Einstein Telescope Meeting, 1–3 March 2010, Friedrich-Schiller-Universität Jena, Jena, Germany.
32. Granata M *et al.* 2013 Cryogenic measurements of mechanical loss of high-reflectivity coating and estimation of thermal noise. *Opt. Lett.* **38**, 5268–5271. (doi:10.1364/OL.38.005268)
33. Hirose E *et al.* 2014 Mechanical loss of a multilayer tantala/silica coating on a sapphire disk at cryogenic temperatures: toward the KAGRA gravitational wave detector. *Phys. Rev. D* **90**, 102004. (doi:10.1103/PhysRevD.90.102004)
34. van Veggel A-MA (on behalf of the LIGO Scientific Collaboration). 2018 Quasi-monolithic mirror suspensions in ground-based gravitational-wave detectors: an overview and look to the future. *Phil. Trans. R. Soc. A* **376**, 20170281. (doi:10.1098/rsta.2017.0281)
35. Pinard L *et al.* 2017 Mirrors used in the LIGO interferometers for first detection of gravitational waves. *Appl. Opt.* **56**, C11–C15. (doi:10.1364/AO.56.000C11)
36. Harry GM *et al.* 2007 Titania-doped tantala/silica coatings for gravitational-wave detection. *Class. Quantum Gravity* **24**, 405–415. (doi:10.1088/0264-9381/24/2/008)
37. Martin IW *et al.* 2010 Effect of heat treatment on mechanical dissipation in $Ta_2O_5$ coatings. *Class. Quantum Gravity* **27**, 225020. (doi:10.1088/0264-9381/27/22/225020)
38. Liu X, White BE, Pohl RO. 1997 Amorphous solid without low energy excitations. *Phys. Rev. Lett.* **78**, 4418–4421. (doi:10.1103/PhysRevLett.78.4418)
39. Steinlechner J. 2017 Optical absorption of aSi coatings from MLD. LIGO Technical report LIGO-T1700545. See https://dcc.ligo.org/T1700545-v1.
40. Steinlechner J, Martin IW, Bassiri R, Bell A, Fejern MM, Hough J, Markosyan A, Route RK, Rowan S. 2016 Optical absorption of ion-beam sputtered aSi coatings. *Phys. Rev. D* **93**, 062005. (doi:10.1103/PhysRevD.93.062005)
41. Schlichtherle S, Strauss GN, Tafelmaier H, Huber D, Pulker HK. 2005 Reactive low voltage ion plating (RLVIP). *Vakuum in Forschung und Praxis* **17**, 210–217. (doi:10.1002/vipr.200500256)
42. Steinlechner J, Khalaidovski A, Schnabel R. 2014 Optical absorption measurement at 1550 nm on a highly reflective $Si/SiO_2$ coating stack. *Class. Quantum Gravity* **31**, 105005. (doi:10.1088/0264-9381/31/10/105005)
43. Steinlechner J, Martin IW, Bell AS, Hough J, Fletcher M, Murray PG, Robie R, Rowan S, Schnabel R. In preparation. Silicon-based optical mirror coatings for ultra-high precision metrology and sensing.
44. Tornasi Z. 2017 Optical properties of silicon for cryogenic GW detectors. In *Proc. of the 12th Edoardo Amaldi Conf. on Gravitational Waves, Pasadena, CA, 9–14 July 2017*. See https://dcc.ligo.org/public/0142/G1700998/001/Z_Tornasi_Amaldi12_SiliconTalk.pdf.
45. Liu X, Queen DR, Metcalf TH, Karel JE, Hellman F. 2014 Hydrogen-free amorphous silicon with no tunneling states. *Phys. Rev. Lett.* **113**, 025503. (doi:10.1103/PhysRevLett.113.025503)
46. Parisi G, Sciortino F. 2013 Structural glasses: flying to the bottom. *Nat. Mater.* **12**, 94–95. (doi:10.1038/nmat3540)
47. Pan HW, Kuo L-C, Huang S-Y, Wu M-Y, Juang Y-H, Lee C-W, Chen H-C, Ting Wen T, Chao S. 2017 Silicon nitride films fabricated by plasma enhanced chemical vapor deposition method for coatings of the laser interferometric gravitational waves detector. *Phys. Rev. D* **97**, 022004. (doi:10.1103/PhysRevD.97.022004)

48. Chao S, Pan H, Kuo L, Huang S, Wu M, Juang Y, Lee C. 2016 Silicon-nitride films deposited by PECVD method on silicon substrate for next generation laser interference gravitational wave detector. In *Optical Interference Coatings 2016, Tucson, AZ, 19–24 June 2016*. OSA Technical Digest (online), paper MB.12. Washington, DC: Optical Society of America.
49. Kuo L, Pan H, Lin C, Chao S. 2016 Cryogenic losses for titania, silica, silicon nitride films and silicon substrates. LIGO Technical Document LIGO-G1601703. See https://dcc.ligo.org/DocDB/0128/G1601703/003/LVC%20poster%20fin.pdf.
50. Steinlechner J, Krüger C, Martin IW, Bell A, Hough J, Kaufer H, Rowan S, Schnabel R, Steinlechner S. 2017 Optical absorption of silicon nitride membranes at 1064 nm and at 1550 nm. *Phys. Rev. D* **96**, 022007. (doi:10.1103/PhysRevD.96.022007)
51. Steinlechner J, Martin IW, Krueger C, Hough J, Rowan S, Schnabel R. 2015 Thermal noise reduction and absorption optimisation via multi-material coatings. *Phys. Rev. D.* **91**, 042001. (doi:10.1103/PhysRevD.91.042001)
52. Yam W, Gras S, Evans M. 2015 Multimaterial coatings with reduced thermal noise. *Phys. Rev. D* **91**, 042002. (doi:10.1103/PhysRevD.91.042002)
53. Steinlechner J, Martin IW. 2016 High index top layer for multimaterial coatings. *Phys. Rev. D* **93**, 102001. (doi:10.1103/PhysRevD.93.102001)
54. Pan HW, Wang SJ, Kuo LC, Chao S, Principe M, Pinto IM, DeSalvo R. 2014 Thickness-dependent crystallization on thermal anneal for titania/silica nm-layer composites deposited by ion beam sputter method. *Opt. Express* **22**, 29 847–29 854. (doi:10.1364/OE.22.029847)
55. Anderson OL, Bommel HE. 1955 Ultrasonic absorption in fused silica at low temperatures and high frequencies. *J. Am. Ceram. Soc.* **38**, 125–131. (doi:10.1111/j.1151-2916.1955.tb14914.x)
56. Cannelli G, Cantelli R, Cordero F, Trequattrini F, Ferretti M. 1996 Strong dependence on doping of a low-activation-energy relaxation process in $YBa_2Cu_3O_{6+x}$: possible polaron relaxation. *Phys. Rev. B*, **54**, 15 537–15 542. (doi:10.1103/PhysRevB.54.15537)
57. Cole GD, Zhang W, Martin MJ, Ye J, Aspelmeyer M. 2013 Tenfold reduction of Brownian noise in high-597 reflectivity optical coatings. *Nat. Photonics* **7**, 644–650. (doi:10.1038/nphoton.2013)
58. Lin AC *et al.* 2015 Epitaxial growth of GaP/AlGaP mirrors on Si for low thermal noise optical coatings. *Opt. Mater. Express* **8**, 1890–1897. (doi:10.1364/OME.5.001890)
59. Cumming AV *et al.* 2015 Measurement of the mechanical loss of prototype GaP/AlGaP crystalline coatings for future gravitational wave detectors. *Class. Quantum Gravity* **32**, 035002. (doi:10.1088/0264-9381/32/3/035002)
60. Murray PG *et al.* 2017 Cryogenic mechanical loss of a single-crystalline GaP coating layer for precision measurement applications. *Phys. Rev. D* **95**, 042004. (doi:10.1103/PhysRevD.95.042004)
61. Cole GD. 2012 Cavity optomechanics with low-noise crystalline mirrors. In *Proc. SPIE 8458, Optics & Photonics, Optical Trapping and Optical Micromanipulation IX, San Diego, CA, 12–16 August 2012* (eds K Dholakia, GC Spalding). Bellingham, WA: SPIE.
62. Steinlechner J, Martin IW, Bell A, Cole G, Hough J, Penn S, Rowan S, Steinlechner S. 2015 Mapping the optical absorption of a substrate-transferred crystalline AlGaAs coating at 1.5 µm. *Class. Quantum Gravity* **32**, 105008. (doi:10.1088/0264-9381/32/10/105008)
63. Cole GD *et al.* 2016 High-performance near- and mid-infrared crystalline coatings. *Optica* **6**, 647–656.
64. Lin AC, Bassiri R, Omar S, Markosyan AS, Lantz B, Route R, Byer RL, Harris JS, Fejer MM. 2015 Epitaxial growth of GaP/AlGaP mirrors on Si for low thermal noise optical coatings. *Opt. Mater. Express* **5**, 1890–1897. (doi:10.1364/OME.5.001890)